Fractal properties of the stretch-twist-fold magnetic dynamo

Samuel I. Vainshtein,[1] Roald Z. Sagdeev,[2] Robert Rosner,[1] and Eun-Jin Kim[3]
[1]*Department of Astronomy and Astrophysics, University of Chicago, Chicago, Illinois 60637*
[2]*East West Space Science Center, University of Maryland, College Park, Maryland 20742-3280*
[3]*The Enrico Fermi Institute, University of Chicago, Chicago, Illinois 60637*
(Received 19 December 1995)

This paper presents direct numerical simulations of the stretch-twist-fold (STF) dynamo. For more than two decades, this dynamo has been viewed as the prototype of the fast dynamo process; and because of its apparently conceptual simplicity, it was generally not thought to be necessary to investigate its quantitative properties in detail via numerical simulations. Furthermore, it has been generally assumed that the STF dynamo is not characterized by small-scale fluctuations, as is usually the case for many other dynamo processes. Numerical simulations show, however, that the STF dynamo process is accompanied by the generation of small-scale fluctuations in the magnetic field. Therefore, it cannot be taken as an *a priori* given that the STF dynamo is a large-scale dynamo; however, our results suggest that the STF dynamo does generate large-scale magnetic fields. In any eventuality, the magnetic fields generated by the STF process do not behave as was previously expected: As we show, these fields become chaotic, first, in the sense that magnetic field lines acquire multifractal properties; and, second, because the field itself becomes chaotic [i.e., the (intermittency) fractal dimensions are no longer trivial]. [S1063-651X(96)08905-2]

PACS number(s): 05.45.+b, 52.30.−q, 47.52.+j, 47.53.+n

I. INTRODUCTION

Since the stretch-twist-fold (STF) magnetic dynamo model was introduced by Vainshtein and Zel'dovich [1], it has become a paradigm for the ''fast dynamo'' process [2]. Conceptually extremely simple, the STF process has appeared to be so intuitively obvious in its functioning that essentially no efforts have been made to study its detailed behavior via numerical simulations. (Thus, although, strictly speaking, the STF process is inherently three dimensional, it has not been difficulties in solving the equations numerically that has prevented further progress. Indeed, in the high conductivity limit, when diffusion may be neglected, the kinematic dynamo problem is exactly solvable via the Cauchy solution; see e.g., [2,3]). In this paper, we provide numerical simulations of the STF process, with the quite unexpected result that the conceptual simplicity of the mechanism turns out to disguise a remarkable complexity of the actual solutions.

One of the goals of this paper is to study the origins of this complexity, which appears to be intimately connected with the generation of small-scale magnetic fluctuations (cf. [4–7] and the review in [1]). This growth of fluctuations is associated with spatial scale reduction of the ambient magnetic fields during the course of magnetic field amplification, down to the diffusive spatial scales. In classical dynamo theory, this process of scale reduction (a concept borrowed from turbulence theory) is essential to magnetic field amplification: only when such scale reduction down to the diffusive scales occurs does the magnetic dynamo (or production of additional magnetic field lines) function [4–7]. In this model, the energy of magnetic fields, $B^2/8\pi$, is concentrated on very small diffusive scales during the field amplification process; these small-scale fields may be called ''fluctuations,'' as opposed to the large-scale component B_0. This means that the ratio $\langle B^2\rangle/\langle B_0^2\rangle$ can become large during dynamo action; for example, in [8] it is assumed that this ratio scales as the magnetic Reynolds number R_m to some power [9],

$$\frac{\langle B^2\rangle}{\langle B_0^2\rangle}\sim R_m^n. \tag{1}$$

If the exponent n is not very small, then this model suggests that the generation of the large-scale magnetic field component might be strongly inhibited for the following reasons: first, the magnetic energy cannot substantially exceed the kinetic one; second, the total magnetic energy largely resides in the fluctuations. As a consequence, there might exist serious restrictions on astrophysical nonlinear magnetic dynamos, the astrophysical problem being that such dynamos are to generate large scale fields, instead of fluctuations on diffusive scales.

Now, simple considerations suggest that the exponent n is of order of unity: For the two-dimensional case, $n=1$ [5], and might be even $\gtrsim 1$ for three dimensions [8]; this conjecture is supported by various calculations, including numerical simulations [10]. Hence the concern regarding the existence of astrophysically interesting magnetic dynamos is hardly settled.

Unfortunately, there are few universally agreed upon results in this subject area. It is suspected that scale reduction to the diffusive scales, and the associated fluctuation growth, is typical behavior; however, one cannot prove that this typical behavior is in fact universal. Consider the conceptually simplest case, namely the kinematic regime, for which one can formulate an eigenvalue problem for the special case of a steady velocity. If we assume an absence of scale reduction (and in the presence of magnetic field growth), then one would expect that, in this simplified case, the scale of the unstable eigenfunctions is comparable to that of the velocity field. However, as shown by Moffatt and Proctor [11],

smooth eigenfunctions do not exist as $R_m \to \infty$. This suggests that, for finite R_m, the eigenfunctions are instead characterized by the diffusive scale $\delta = l/R_m^{1/2}$ (l is the characteristic scale of the velocity field); and that $\delta \to 0$ as $R_m \to \infty$ [11]. This in turn suggests that the initially ''smooth,'' (i.e., large-scale) field adjusts to the eigenfunction with largest growth rate, i.e., decreases its spatial scale until it reaches the diffusive size scale δ.

These issues, which have been addressed for some time in dynamo literature, were not in fact discussed in the context of the STF process; indeed, it has been conjectured that the exponent n in (1) is small, or even zero, for the STF mechanism [3], e.g., that there is growth of magnetic flux on large scales, but not on the small spatial scales of fluctuations. This circumstance gave rise to the hope that the STF process might resolve the perceived difficulties with astrophysical dynamos; see, e.g., [3,12–14]. This hope is countered by the objection that the Moffatt-Proctor theorem on eigenfunction singularity for the limit $R_m \to \infty$ does not apply here because the motion associated with the STF process is *not* steady. As we will show by direct numerical simulation, the STF process does lead to small-scale fluctuations in the magnetic field; we therefore might speculate that because the STF motion is periodic (a circumstance which leads to Floquet-type eigenfunctions), a properly modified version of the Moffatt-Proctor theorem might nevertheless apply.

In this paper, we shall revisit the STF process, and using both analytical and numerical tools, will address three questions.

(i) Is there a large-scale dynamo associated with the STF process; in particular, is there generation of large-scale magnetic flux via the STF process?

(ii) Do fluctuations appear in the course of STF action?

(iii) If the answer to the second point is positive, then is there also a small-scale dynamo process acting during the STF? (A small-scale dynamo is a process in which the scale reduction is accompanied by magnetic field amplification, such that the scale-reduction process is less efficient than the magnetic field amplification [1].)

The paper is thus organized as follows. After formulating the basics in Sec. II, we describe the STF process that gives rise to fast dynamo action (Sec. III). The results of the simulations are described in Secs. IV and V; Sec. IV is devoted to a discussion of the numerical methods used by us to follow the evolution of magnetic field lines (which might be easily modified to solve a variety of other fluid-dynamics problems), while the spatial correlation of the magnetic field will be examined in Sec. V. Our summary and conclusions are provided in Sec. VI.

II. FORMULATION OF THE PROBLEM

We are looking for (exponentially) growing solutions of the induction equation

$$\frac{\partial \mathbf{B}}{\partial t} = \boldsymbol{\nabla} \times [\mathbf{u} \times \mathbf{B}] + \eta \boldsymbol{\nabla}^2 \mathbf{B}, \tag{2}$$

where the velocity field $\mathbf{u}$ is defined by the equation of motion

$$\frac{\partial \mathbf{u}}{\partial t} + (\mathbf{u} \cdot \boldsymbol{\nabla})\mathbf{u} = -\frac{\boldsymbol{\nabla} p}{\rho} + \frac{1}{4\pi\rho}[\nabla \times \mathbf{B}] \times \mathbf{B} + \nu \nabla^2 \mathbf{u} + \mathbf{F}, \tag{3}$$

where $\mathbf{F}$ are external forces stirring the conductive medium.

The viscosity ν and diffusivity η are small for most astrophysically interesting cases (i.e., we have both the Reynolds number $R \gg 1$, and the magnetic Reynolds number $R_m \gg 1$). This circumstance makes it very difficult, if not impossible, to solve Eqs. (2) and (3) in the fully general case. Even in the kinematic regime (when back reactions of magnetic fields on the motion are ignored), for which the velocity field is considered to be given, there is no general solution of (2) known. This situation is aggravated by the fact that the magnetic-field energy grows mostly on diffusive scales, so that the Lorentz back reaction is already present when the large-scale magnetic-field component (which we are interested in from the astrophysical point of view) is really very weak [10]. In other words, the nonlinear nonkinematic regime comes into play very early on in the generation of magnetic fields, and therefore the kinematic approach becomes invalid. Below, we will follow the ''post-kinematic'' approach suggested by Childress and Gilbert [3], which focuses primary attention on the role of magnetic fluctuations in modifying the fluid flow, and their impact on the dynamo.

The first issue we address is whether fluctuations can appear in the STF model. If magnetic field amplification during the STF process is *not* accompanied by scale reduction in the magnetic field (i.e., not accompanied by generation of strong magnetic fluctuations), then we obtain the results expected for the past 20 years, i.e., a large-scale dynamo. If, however, magnetic fluctuations do appear, then there still remains the question of whether large-scale magnetic fields are generated. If fluctuations *are* present, then the question is whether the amplification of magnetic fields due to line stretching is more effective than the scale reduction [point (iii) of Sec. I].

In order to address these issues, we will solve Eq. (2) numerically, for the ideal case $\eta = 0$ ($R_m \to \infty$). We first note that there is an exact solution to this equation, namely the Cauchy solution

$$B_i(\mathbf{x},t) = B_j^{(0)} \frac{\partial x_i}{\partial a_j}, \tag{4a}$$

$$\mathbf{B}^{(0)} = \mathbf{B}(\mathbf{a}(\mathbf{x},t),0), \tag{4b}$$

where $\mathbf{a}(\mathbf{x},t)$ is the initial ($t=0$) position of a Lagrangian trajectory that arrives at point $\mathbf{x}$ at time t. A conceptually simple approach to obtain the solution is to rewrite Eq. (4) in terms of the Lundquist solution (see e.g., [15,12])

$$\frac{\mathbf{B}(\mathbf{x},t)}{B(\mathbf{a})} = \frac{d\mathbf{s}}{ds(t=0)}, \tag{5}$$

where $d\mathbf{s}$ is an infinitesimal vector connecting two neighboring liquid particles. The procedure for computing the magnetic field evolution in time is straightforward: Suppose we are given a flow ($\dot{x} = u_x$, $\dot{y} = u_y$, and $\dot{z} = u_z$), and suppose further that we will examine the evolution of a given magnetic field line, whose location is specified at time $t=0$. If we discretize the field line, i.e., approximate the field line by a

finite number of short straight line segments $d\mathbf{s}$ joining sequential points on the magnetic field line, then the evolution of the field line is defined by the motion of these line segments.

Specifically, consider the ith line segment: its ends are defined at any given time by

$$d\mathbf{s}_i=\{\mathbf{x}_i(\mathbf{a}_i,t),\mathbf{x}_{i+1}(\mathbf{a}_{i+1},t)\},$$

where $\mathbf{a}_i$ and $\mathbf{a}_{i+1}$ are the initial ($t=0$) position of the tth infinitesimal line segment. With the use of actual flow expressions

$$(\dot{x}=u_x,\dot{y}=u_y,\dot{z}=u_z),$$

one can now solve for the Lundquist solution (5) by appropriate simple substitution for the velocity flow.

III. STF VELOCITY FIELD

We use an analytical form of the STF, suggested by Moffatt and Proctor [11]. The velocity is presented as a combination of polynomials of lowest possible orders. In order to make sure that the motion is bounded at infinity, the vector potential of this velocity is multiplied by the exponential term $\exp\{-\mathbf{x}^2/R^2\}$; this insures that the velocity goes to zero at infinity.

The first step, ''stretch,'' is described by

$$\hat{S}:\quad \mathbf{u}_1=a_1e^{-\mathbf{x}^2/R_1^2}(x-2xz^2/R_1^2,y-2yz^2/R_1^2,-2z+2(x^2+y^2)z/R_1^2). \tag{6}$$

This velocity stretches all field lines not far from the $z=0$ plane, and (because of the assumed damping exponent, or requirement that the motion is bounded) leads to the opposite process on the periphery, namely compression of field lines. Therefore, we have to restrict ourselves to regions not far from $z=0$.

Next, we make a figure ''eight'' from the loop, compressing it along the y axis [16],

$$\hat{T}_1:\quad \mathbf{u}_2=a_2e^{-x^2/R_2^2-(y^2+z^2)/r_2^2}(0,-y+2yz^2/r_2^2,z-2zy^2/r_2^2). \tag{7}$$

The next step is to twist about the x axis, described by

$$\hat{T}_2:\quad \mathbf{u}_3=a_3e^{-\mathbf{x}^2/R_3^2}(0,\omega(x)z-xz(y^2+z^2)/R_3^2,-\omega(x)y+xy(y^2+z^2)/R_3^2), \tag{8a}$$

$$\omega(x)=x. \tag{8b}$$

Now the loop should lie in the XZ plane, and we want to fold it in the y direction. This can be accomplished by the motion

$$\hat{F}:\quad \mathbf{u}_4=a_4e^{-y^2/R_4^2-(x^2+z^2)/r_4^2}(-x+2(xy^2+cx^3y)/R_4^2,y+3cx^2-2(x^2y+cx^4)/r_4^2,0). \tag{9}$$

We end up with a loop in the YZ plane, centered at some positive value of y (and $x=z=0$). We have to shift it back, so that the center is at $y=0$, and turn it about the y-axis [17].

As a final aside regarding this STF flow, we note that there are 11 distinct parameters which define this flow: a_1, a_2, a_3, a_4, r_2, r_4, R_1, R_2, R_3, R_4, and c.

IV. NUMERICAL SIMULATIONS

In this section, we discuss the results obtained by solving Eqs. (5) numerically, based on the use of the STF flow (6)–(9). These simulations suggest that the simple picture of the STF dynamo applies only to a set of field lines of measure zero, i.e., that virtually all field lines subjected to the STF flow experience transformations that lead to field line chaos. An essential question is whether this result hinges on an ''appropriate'' choice for the flow parameters which enter into the definition of the analytical STF flow (6)–(9), i.e., whether—with a more judicious choice of these parameters—one in fact could recover the simple picture for the STF dynamo process for almost all field lines. As we will see (in Sec. IV B), this question can be answered in the negative for continuous motion.

A. Mapping of magnetic field lines

In Sec. III, we described the technique used by us to implement the STF flow numerically, namely by using the Lundquist solution (5); in this subsection, we provide some illustrative examples of the effects of this flow on field line geometry as these magnetic field lines are deformed by the flow (6)–(9).

The illustrations we focus on all start with the topologically simplest magnetic field geometry, namely circular (closed) field lines placed at various locations with respect to the origin. Two distinct sets of calculations will be displayed. The first set [case A] consists of 64×65 concentric coplanar circles (ranging in radius ρ from 0 to 1), where the common plane is specified parametrically by ($z=h$, $h=$const), and where we shall let $z=h$ lie in the value range $-0.5\leqslant h\leqslant 0.5$ (or $-0.5/\pi\leqslant h\leqslant 0.5/\pi$); this gives 65 distinct values of h. The second set of calculations [case B] focuses on a single (initially circular and planar) field line, whose center lies in the planes $z=0$ or $z=0.1$.

The difference between these two sets of calculations is largely in the resolution of the numerical solution (e.g., in the number of points taken on any given initial closed field line), and whence in the duration for which the Lundquist solution can be followed sensibly without significant loss of geometric information [18]. In particular, the first set of calculations entails taking 64 points per initial field line (i.e., an interpoint distance of $\pi/64$), while the second set of calculations entails taking 64^3 points per initial field line (i.e., an interpoint distance of $\pi/64^3$). Thus we can follow the field line distortion for far longer durations in the second case than in the first. In particular, the average distance between adjacent points on a given field line for case A becomes comparable to unity after only two STF cycles; hence, only a single STF cycle can be sensibly followed in this set of calculations. However, as we show immediately below, this is sufficient to demonstrate (both qualitatively and quantitatively) the sensitivity of the geometric field line distortions on the precise initial location

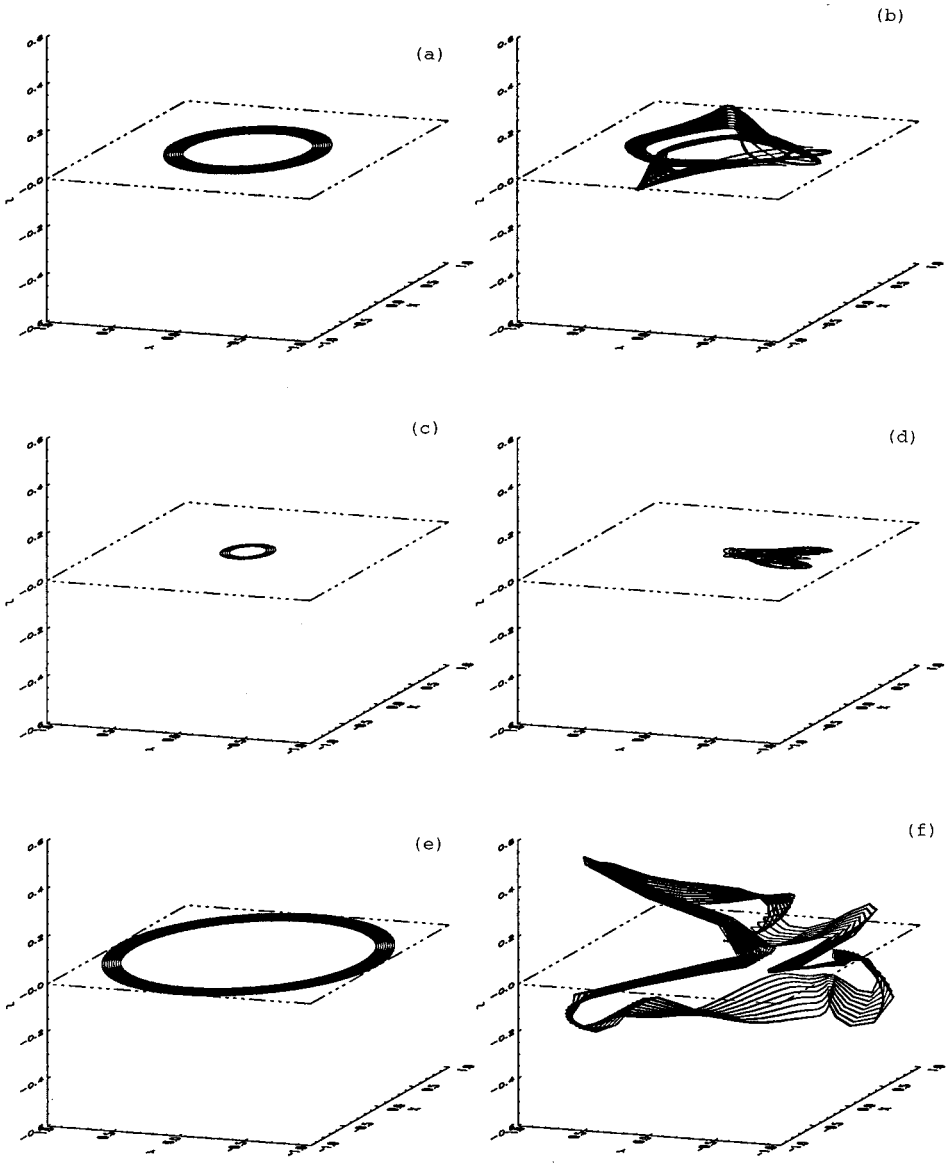

FIG. 1. Evolution of a bundle of magnetic field lines after one STF cycle (case *A*). Initial lines (left-hand panels) are placed in the vicinity of the $z=0$ plane, with radius $r=0.51$ (a), $r=0.2$ (c), and $r=0.9$ (e). The corresponding final field line bundles are shown in (b), (d), and (f), respectively. The parameters for the STF are $a_1=1.3$, $a_2=3.0$, $a_3=3.30$, $a_4=1.0$, $r_2=1.0$, $r_4=0.7$, $R_1=1.0$, $R_2=0.3$, $R_3=0.71$, $R_4=1.4$, and $c=1.9$.

of a given ''test field line.'' In case *B*, our resolution criterion allows us to compute the geometric distortion of the single field line for up to six STF cycles; again, we will shortly show that even though we now follow only a single field line, the computation suffices to apply quantitative analyses to the resulting complex geometric object. In particular, the Hausdorff dimension of the line is shown to be greater than 1.

We begin our illustrations with case *A*: Fig. 1 depicts the evolution of three bundles (or tubes) of magnetic field lines lying in the plane $z=0$ as a result of one STF cycle; the figure shows selected lines, whose radii lie in the vicinity of $\rho\sim0.51$ (upper panel), $\rho\sim0.2$ (middle panel), and $\rho\sim0.9$ (lower panel). While the flux tube with $\rho\sim0.51$ seems to deform roughly as expected from the STF transformation, this is not the case for the other two flux tubes: the field lines with initially smaller radii are simply compressed (see the explanation below in Sec. IV B), while the initial field lines with initially larger radii are highly distorted in an apparently random manner.

Magnetic flux tubes which lie only slightly out of the plane $z=0$ behave completely differently. In Fig. 2 we show the evolution of three additional cases, now for fixed ρ $(=0.51)$, but varying initial plane. It is evident that in no case do we obtain a geometric result after one flow cycle which resembles the canonical STF picture of field line distortion.

In order to illustrate that repeated application of the STF flow enormously complicates the resulting field line geometry, we have followed the time history of a single field line (case *B*) as well; as already alluded to, the focus on a single field line affords additional computational power, from which comes the ability to follow the field line evolution further in time.

To make our point, let us consider the temporal evolution of those field lines that most closely conform to expectation after one STF cycle, i.e., they are ''properly behaved.'' As shown in Figs. 3 and 4, although these field lines are relatively rare, they do exist. We suspect that it is the *continuous* nature of the STF transformation (6)–(9) that leads to this situation.

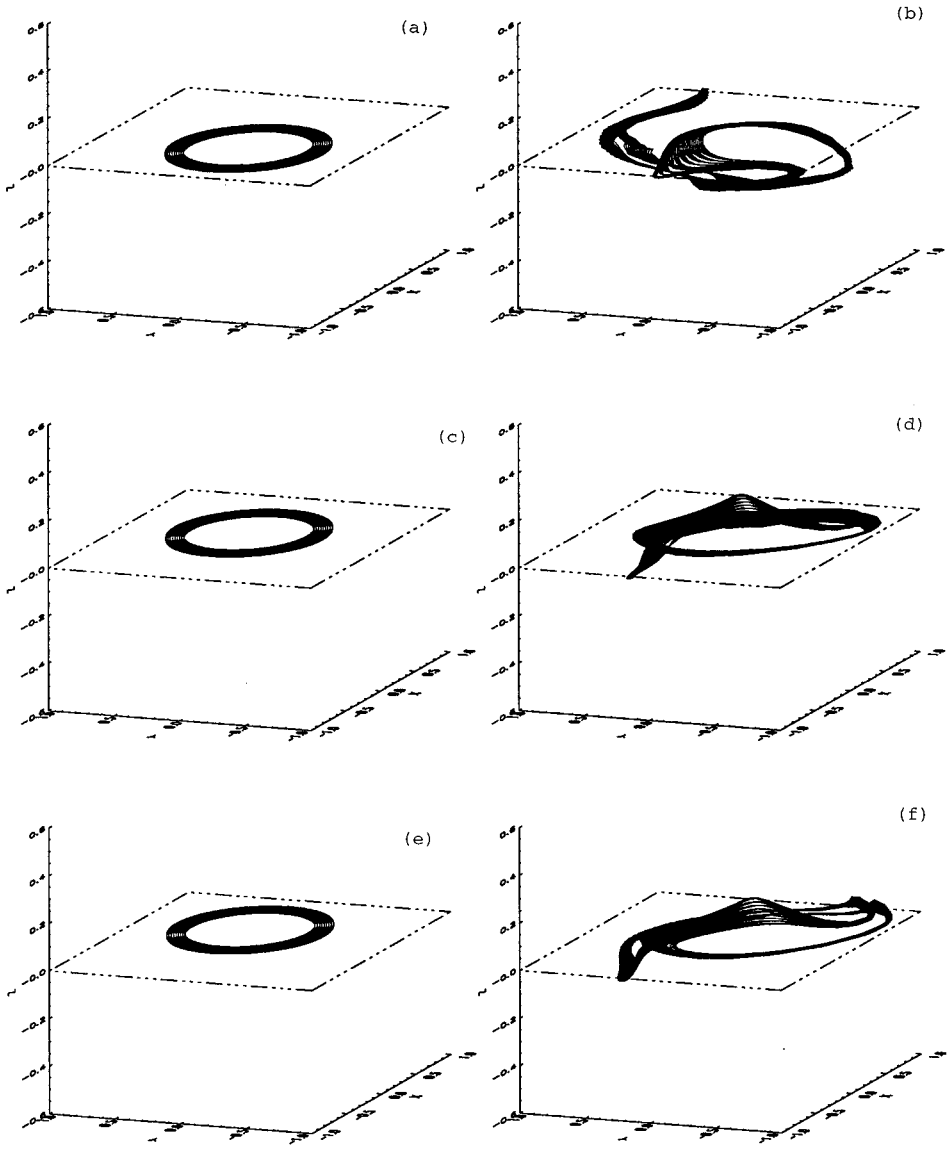

FIG. 2. Same as Fig. 1, but with fixed initial flux tube radius ($\rho \sim 0.51$) and varying initial plane: $z=-0.01$ (a), 0.01 (c), and 0.1 (e); the final flux tube configuration after a single STF transformation is shown in (b), (d), and (f), respectively.

However, Fig. 3 also shows that the actual geometrical distortion of such a ''properly behaved'' field line after the initial STF cycle is not perfect; that is, there are small discrepancies between the actual distorted field line and the ''ideal'' STF, processed field line [cf. Figs. 1(b) and 3(b)]. The key point that Fig. 3 demonstrates is that it is these small discrepancies that lead to ultimate field line chaos even for these ''well-behaved'' field lines.

A second case ($z=0.1$ at $t=0$) is shown in Fig. 4. It is evident that even after a single STF cycle, the field line deformation is already geometrically complex; as time proceeds, complexity grows yet greater—there is some resemblance to the Lyapunov exponential separation of two neighboring particles in a chaotic flow. (We will pursue this aspect further quantitatively in Sec. IV B.)

B. Parameter sensitivity

An obvious and very important question following from the results just obtained is whether these results are just an unfortunate consequence of a particular choice of the parameters defining the initial field line configuration (i.e., $z=h$ and ρ) or of the 11 parameters characterizing the STF flow; or whether these results are really a generic description for this type of flow. In other words, could a more judicious choice of control parameter space avoid these difficulties? We have in fact explored the full parameter space to some extent (for obvious reasons, a high-resolution study of this 11-dimensional space could not be carried out). In no case did we find a preponderance of ''well-behaved'' field lines after one STF cycle; generally, only a small fraction (of the order of a few percent) of the initial field lines behaves ''properly.''

To be more specific, let us consider the actual sequence of transformations embodied in the STF. We find that virtually any combination of control parameters leads to a successful stretch $\hat{S}$ operation (i.e., essentially all field lines are ''well behaved'' after the $\hat{S}$ operation). However, this is not true for the next twist operation. Consider the transformation $\hat{T}_1$ [Eq. (7)]: One obtains ''figure eight'' loops only for field lines whose initial radius ρ is, roughly speaking, greater than R_2; field lines whose initial radius is comparable to, or smaller than, R_2 would be simply compressed to the x axis, see Fig.

1(d). The next step, ''twisting'' of the field lines ($\hat{T}_2$) is even more complicated, because the ''angular velocity'' ω is a function of x. Thus, for any given time allotted for this stage, only ''selected'' loops halves would turn sufficiently so that the entire loop is twisted 180°; loops of smaller size, and therefore, with smaller angular velocity, would not have sufficient time to finish the 180° twisting, while larger loops would be overtwisted, i.e., twist more than 180°.

Thus we are left with only few percent of the field lines that behave ''properly.'' We found that very careful parameter tuning is required to do the next step, folding $\hat{F}$, for these few ''selected'' field lines, otherwise they are distorted

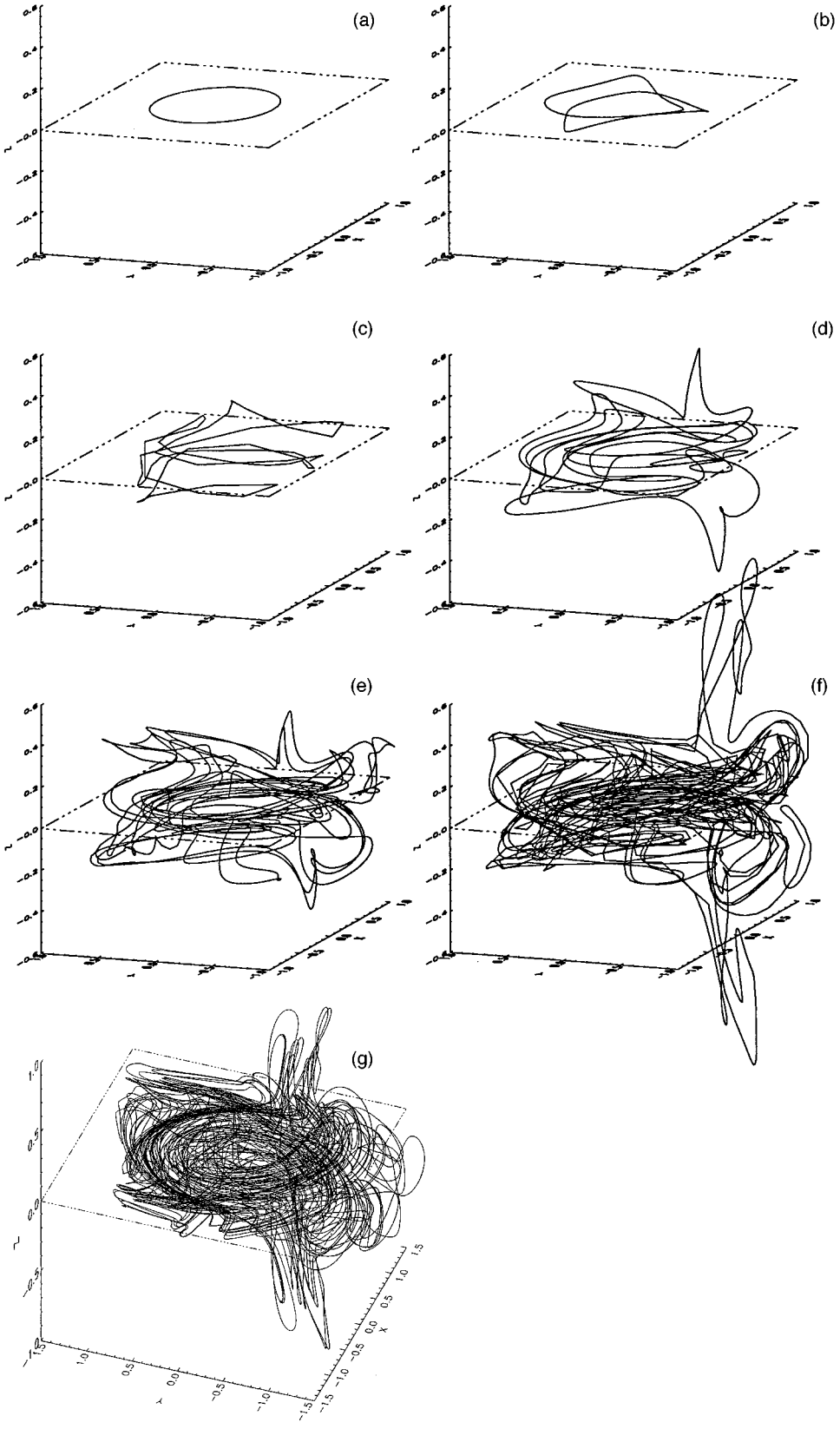

FIG. 3. Evolution of a single field line (case B), lying in the plane $z=0$. Time is measured in terms of the number of STF cycles. (a) Initial line ($t=0$). (b) $t=1$. (c) $t=2$. (d) $t=3$. (e) $t=4$. (f) $t=5$. (g) $t=6$.

and deformed in unpredictable way. This suggests that if a special choice of control parameters exists that yields a fraction of ''well-behaved'' field lines, then it must occupy a small fraction of the phase space volume. Finally, as mentioned in Sec. IV A, even selected field lines do not form perfect double circles.

Thus we arrive at two conclusions. First, the analytical representation of the STF transformation accomplishes the geometric field line distortions traditionally associated with the stretch-twist-fold dynamo only for a few ''selected'' field lines; essentially all other field lines are transformed in an apparently chaotic manner. Second, even these ''selected'' field lines, which behave ''well'' (or as well as could be) after one STF cycle, behave ''badly'' (i.e., do not conform to the traditional STF picture) for subsequent STF cycles.

C. Fractal dimensions of stretched magnetic field lines

The initial geometry of the field lines we have studied has been kept simple, and thus smooth. The question we now address is whether successive STF transformations lead to a geometrically more ''complex'' field line object.

To begin with, we note that for any finite number of successive STF cycles, a given field line must remain smooth, e.g., its topological dimension remains equal to 1. Thus any departures from smoothness in this sense can only be regarded in an asymptotic sense, as the number of successive STF cycles goes to infinity. Nevertheless, we are able to ask whether neighboring points on a given field line exhibit scaling as the number of successive STF cycles increases (but is still finite); such emergence of scaling behavior will be regarded by us as evidence of the appearance of field line chaos. In particular, we shall ask whether the curve defined by a stretched field line has fractal length, and whether this curve shows evidence of multifractal structure. In order to attack this problem, we shall use the expression [19]

$$\left\langle \left(\frac{\Delta\Lambda}{\Delta s} \right)^q \right\rangle \sim \left(\frac{1}{\Delta s} \right)^{\kappa q + (1-D_q)(q-1)}, \tag{10}$$

where $\Delta\Lambda$ is the distance between two points (whose initial separation is given by Δs), and the fractal (or generalized) dimensions are denoted by D_q. Note that by setting $q=1$, we recover the classical definition of the fractal length dimension; thus, if $\langle \Delta\Lambda/\Delta s \rangle$ shows scaling properties, κ can be found. The Richardson-Mandelbrot dimension D is then given by

$$D = 1 + \kappa. \tag{11}$$

[The scaling of $\langle (\Delta\Lambda/\Delta s)^q \rangle$, if any, can be measured for arbitrary q.] For a regular (smooth) curve, $\kappa=0$ and $D_q \equiv 1$; therefore [using Eq. (11)] $D=1$, and the exponent in (10) is zero—this is the trivial case. If the STF transformation would function as was expected (e.g., [1]), then the field line length would double after each cycle, so that after six cycles the field line length would grow to $2^6=64$ times its original length. Each subsegment of this curve would grow in exactly the same way, so that $\langle (\Delta\Lambda/\Delta s)^q \rangle = 64^q$; hence $\langle (\Delta\Lambda/\Delta s)^q \rangle$ *would not scale with* Δs, and therefore the exponent in Eq. (10) is zero: The *expected* (perhaps naive) result from repeated STF transformations therefore reduces to the trivial case just discussed.

Now consider how field lines actually behave when subjected to the STF transformation. First, let us look at the behavior of the dimension D [i.e., at the case $q=1$ in Eq. (10): Figures 5(b) and 5(d) give an evaluation of D for cases we have computed, and we find $D>1$; therefore we do not obtain the trivial case. Next, let us ask for the nature of the magnetic surfaces generated during the STF process, which may be quantitatively described by their dimension: According to the intersection theorem, the dimension of a magnetic surface is given by $D^{(2)}=D+1$ (the Hausdorff dimension $D^{(H)}$ of the set covered by a magnetic surface therefore coincides with $D^{(2)}$ [19]). We find that (in both cases), $D^{(H)}=2.6$, whereas the dimension naively expected from the STF process would be 2.

Another way of looking at this result is to consider the dimension spectrum D_q: Figures 5(a) and 5(c) illustrate scaling for the evolution of a field line which initially lies in the planes $z=h=0$ and $z=h=0.1$, respectively, for a range of values of q. We observe good scaling behavior for about four decades in both cases; the field lines clearly do not behave in the ''trivial'' manner described above. Indeed, evaluation of the dimension spectrum D_q for both cases [Figs. 5(c) and 5(d)] shows strong departure from the ''trivial'' behavior, demonstrating a significant departure from unity for D_q ($q>0$) in both instances. Remarkably, the two dimension spectra are essentially identical if account is taken of the error bars. The highest-order dimensions we have calculated substantially deviate from unity ($D_4=0.75$); there is no evidence that an asymptotic value has been reached (i.e., $D_4>D_q$ for $q>4$). This suggests that the magnetic field becomes stochastic as the STF process proceeds.

The existence of scaling in this field line stretching process suggests the following physical scenario: As usual (cf. [1]), the stretching and shearing of magnetic fields is accompanied by scale reduction. Once the characteristic scale of the field is smaller than that of the motion, the stretching becomes effectively self-similar (because the large scale structure of the motion is no longer relevant). The fact that we see multifractal behavior (e.g., the fact that the generalized dimensions for $q>1$ depart significantly from unity) suggests that the field line stretching is not homogeneous, i.e., that the Lyapunov exponent is different in different places.

D. Details of magnetic field structure

To get a better idea of what the magnetic field looks like as it evolves subject to the STF flow, we show all three components of its components in the XY plane after *one* STF cycle (i.e., case A; Fig. 6). Several important results emerge immediately. First, according to the ''standard'' STF process, the vertical (B_z) field component should remain zero; however, it clearly does not vanish, and instead shows fairly complex geometric structure [Fig. 6(b)]. Similarly, the expectations for the B_z and B_y components is that they essentially retain the same geometric structure as they had at $t=0$; in contrast, Figures 6(c)–6(f) show that while the average geometric structure is indeed retained, the detailed spatial behavior of these two field components is much more complex: There are ''unwanted'' enclaves of opposite polarities

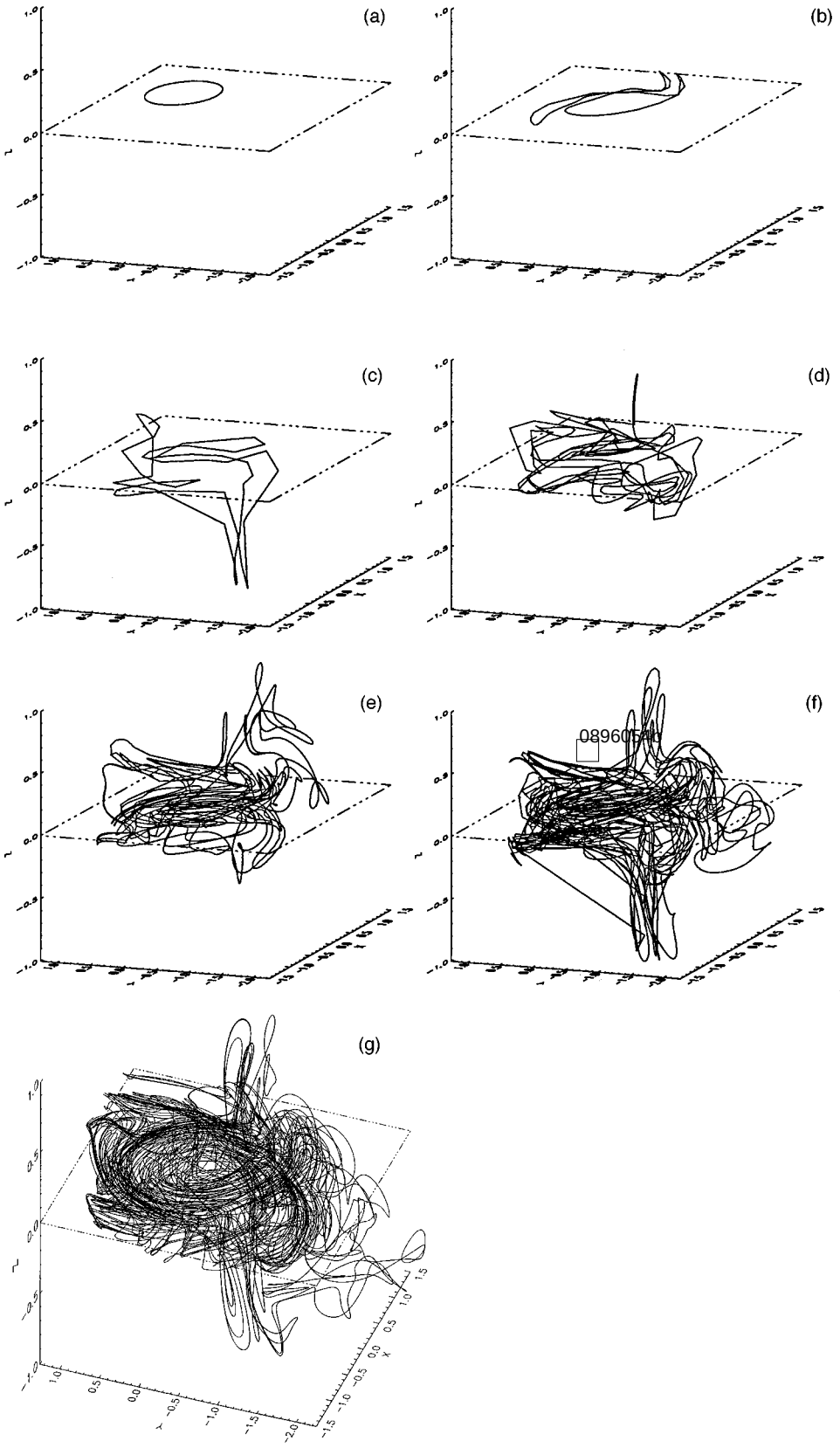

FIG. 4. Same as Fig. 4, but the initial line lies in the plane $z=0.1$.

everywhere (where ''opposite'' means opposite to previous expectations), and the neutral line (which corresponds to the curve separating opposite polarities) is geometrically very complicated. If one looks at the results of the case *B* calculations (for which we obtain the magnetic field portrait after six STF cycles), all evidence of the original geometric field structure is lost: Figure 7 presents all three components of the field (as in Fig. 6) for an initial field line lying in the $z=0$

plane; it is evident that the field is extremely complicated, and does not retain any of the geometric simplicity—even in the mean—expected from the STF process.

V. CORRELATION PROPERTIES OF THE FIELD: IS THERE A DYNAMO?

The next step is to examine the detailed correlation properties of the stretched magnetic field: The standard STF process is thought to lead to amplification of the large-scale field components only, with essentially no fluctuations. Is this in fact correct for the STF process we are studying here? From Sec. IV, we have seen that the answer (at least on the qualitative level) is no: Fluctuations are seen to grow rapidly in our calculations, so that the correlation length ought to decrease dramatically. In order to study this process quantitatively, we will investigate the correlation properties of a single field line for two cases (e.g., when the initial field line is at $z=0$ and at $z=0.1$). As an aside, we note that several aspects of the correlation function have a direct physical interpretation: First, the zero-lag correlation function is just the average magnetic energy $\langle B^2\rangle$; second, the correlation length is a measure of the typical magnetic field line scale; third, the long-range portion of the correlation function is directly relevant to the study of the large-scale magnetic dynamo.

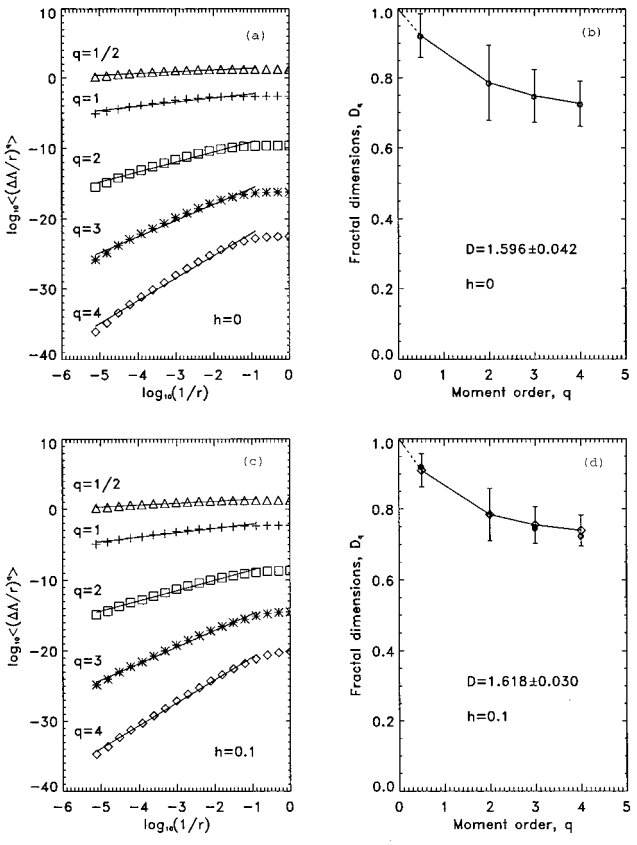

FIG. 5. Multifractal dimensions of magnetic field line length. (a) Scaling for an initial field line lying in the $z=h=0$ plane. (b) Corresponding dimension spectrum D_q. Panels (c) and (d) are the same as (a) and (b), respectively, but the initial field line lies in the $z=h=0.1$ plane. For comparison, we have superimposed generalized dimensions for the $h=0$ case [from (b)] on (d) [using the same symbol as in (b)]; we observe that the two dimension spectra are almost identical.

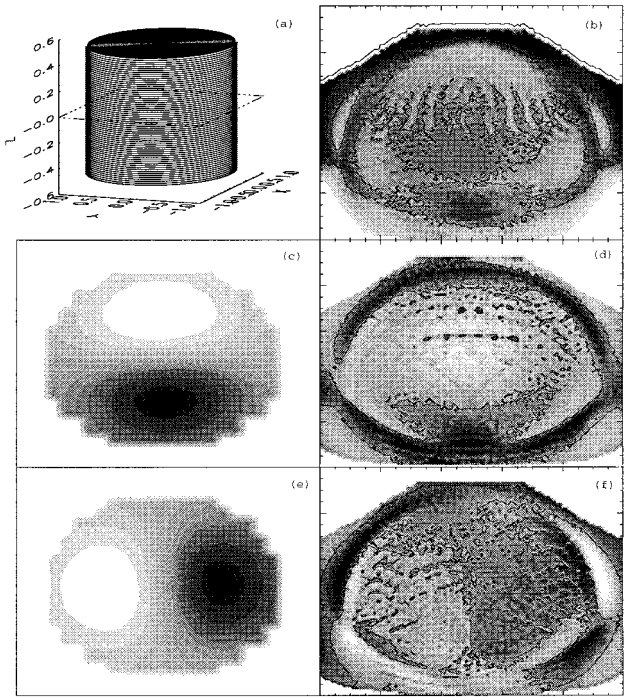

FIG. 6. Mapping of the magnetic field into the XY plane, following one STF cycle; the light (dark) greyscale corresponds to negative (positive) values. (a) Initial field lines are shown as concentric circles, with radii from 0 to 1, lying in 65 planes between $z=-0.5$ and $z=0.5$. (b) Projection of the B_z component into the XY plane. (c) Projection of the initial B_x component. (d) Projection of B_x after one STF cycle. (e) Projection of the initial B_y component. (f) Projection of B_y after one STF cycle. A comparison of the initial ($t=0$) projections with the $t=1$ projections shows that, contrary to naive expectations, the relatively simple geometry of the initial state is not preserved when the STF transformation is applied.

A. Intermittency fractals

We first ask if the fluctuations are chaotic. We calculate correlations of magnitudes, and make use of a formula linking them to fractal dimensions (see [20]),

$$\langle[\mathbf{B}(\mathbf{x}+\mathbf{r})^2\mathbf{B}(\mathbf{x})^2]^{q/4}\rangle \sim r^{(3-D^{(i)}_{q/2})(q/2-1)2-(3-D^{(i)}_q)(q-1)}; \tag{12}$$

here the generalized dimensions $D_q^{(i)}$ are based on the measure

$$\mu(C_i)=\frac{\int_{C_i}|\mathbf{B}|\,d\mathbf{x}}{\int_V|\mathbf{B}|\,d\mathbf{x}},$$

where the total volume V is divided exhaustively into disjoint subsets C_i. Physically, these dimensions test for the presence of intermittency. Figure 8 presents scaling properties for the quantity on the left-hand side of (12). The scaling [Figs. 8(a) and (c)] does not have as large a range of spatial scales as the length-of-line scaling shown in Fig. 5 (e.g., only two and a half decades), but the error bars are substantially smaller than for this previous case. Our results clearly show

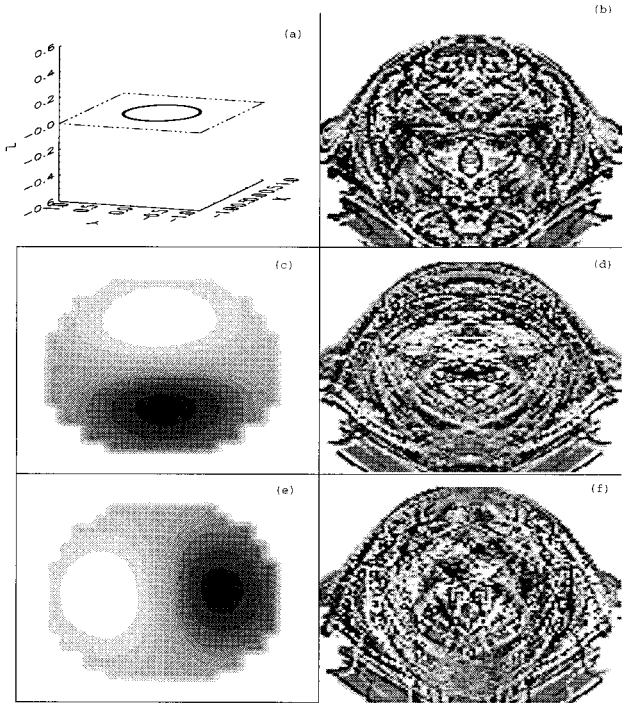

FIG. 7. Mapping of a single field line lying initially in the $z=0$ plane, shown in (a). All other panels are as in Fig. 6, except that the final states of the single field line corresponds to six (6) STF cycles. This figure also demonstrates the point that the naive expectations regarding the geometry of field lines following the STF transformation are not met, but that the field geometry instead becomes increasingly complex with time.

that the field is rather intermittent. Indeed, a rough estimation of intermittency can be obtained via the flatness factor

$$\frac{\langle B^4\rangle}{\langle B^2\rangle^2},$$

whose value needs to be compared with the Gaussian value of 3. From Figs. 8(b) and 8(d), it is clear that this factor is much larger than 3, indicating very strong departure from Gaussian behavior.

A more subtle estimation of intermittency, or intermittency for different scales, is presented by the generalized dimensions. We note first that the $D_q^{(i)}$ values we obtain are definitely not trivial, i.e., $D_q^{(i)}\neq 3$. Second, they are substantially less than 3 (indeed, $D_4^{(i)}<2$), and they do not reach an asymptotic value in the domain in which we carried out the computations. It can be proven that the generalized dimensions decrease with growing q [21]; that is seen in both Figs. 5 and 8. Therefore, the asymptotic value of $D_q^{(i)}$, $D_{q\to\infty}^{(i)}$ must be still smaller; and the measure of multifractality, $3-D_{q\to\infty}^{(i)}$ [20], is larger than 1. Finally, we note that the flatness factor is larger, and the generalized dimensions are smaller, for $h=0.1$ case than for the case $h=0$. We interpret this to mean that the curve for $h=0.1$ is more singular than the curve corresponding to $h=0$. We might have expected that because, at least after the first STF cycle, the line initially starting from the $z=0$ plane is mapped simply into a (slightly distorted) double circle, while the line starting in the $z=0.1$ plane is already geometrically complicated after the first cycle. Summarizing: we see that we obtain multifractal structure both in the length of magnetic line lines (Fig. 5) and in the field intermittency (Fig. 8).

We have already seen in Sec. IV that the evolved magnetic field lines are chaotic. It is well known that the equations defining a field line are equivalent to those describing a trajectory of a dynamical system, and calculations of such trajectories have shown that they become chaotic [22,23]. These calculations typically show that the Lyapunov exponent is positive, and therefore trajectories are chaotic for these flows [22,23]. In addition, we have just shown above that the magnetic field is itself chaotic: this would not necessarily be the case for chaotic trajectories. Indeed, Lagrangian chaos may appear in the case of a regular Eulerian field. Another difference from the previous calculations is that we see a *transition to chaos*. That is, both field lines and the magnetic field are regular at the beginning ($t=0$), but after (only) six STF cycles both become chaotic. Our case is quite similar to that described by Rosenbluth *et al.* [24]: in Rosenbluth *et al.*'s case, chaotic field lines, as well as chaotic magnetic fields, appear from an initial regular state, with straight magnetic field lines. In their case, the perturbations grow exponentially as a result of instabilities, and chaos appears if resonant regions overlap. This differs from our case, where resonant conditions are irrelevant, because our transition to chaos is ''kinematic,'' i.e., induced by the velocity field (which is given, and is represented by, the STF transformations). However, the point here is that the velocity field in our case is *regular*, and nevertheless generates a chaotic magnetic field. Therefore, the transition to chaos is not trivial.

B. Magnetic field correlations

If the STF would work as expected, i.e., if the large-scale flux were to grow exponentially without substantial contributions from fluctuations, then the correlation function would grow self-similarly [13], e.g.,

$$C(\mathbf{r})\equiv\langle\mathbf{B}(\mathbf{x}+\mathbf{r},t)\cdot\mathbf{B}(\mathbf{x},t)\rangle\sim e^{2\gamma t}\langle\mathbf{B}(\mathbf{x}+\mathbf{r},0)\cdot\mathbf{B}(\mathbf{x},0)\rangle. \tag{13}$$

This means that the correlation scale would not decrease.

However, as we have already pointed out, fluctuations *are* generated; and we can ask how $C(\mathbf{r})$ behaves as a result. Figure 9(a) depicts the correlation function at different time steps (measured in units of one STF cycle), for a magnetic field line started in the $z=0$ plane. One can clearly see that the correlation scale decreases, and that the growth of $C(\mathbf{r})$ is not self-similar. Note that, in view of the dramatic growth of the magnetic energy, the plot has been drawn on a logarithmic scale, and therefore the negative parts of the correlation functions cannot be depicted. In fact, on a linear scale, the correlation function can be seen to decrease to zero on a correlation length, and then to fluctuate about zero; this is illustrated in Fig. 9(b), in which we show the correlation function ''tails'' on a linear scale.

At any given time, the correlation function can be fit well by polynomials for lags smaller than the first zero; this allows us to construct a statistically defined correlation length

$$\delta\equiv\lim_{r\to 0}\left|\frac{C(\mathbf{r})}{\frac{1}{2}d^2C/dr^2}\right|^{1/2}.$$

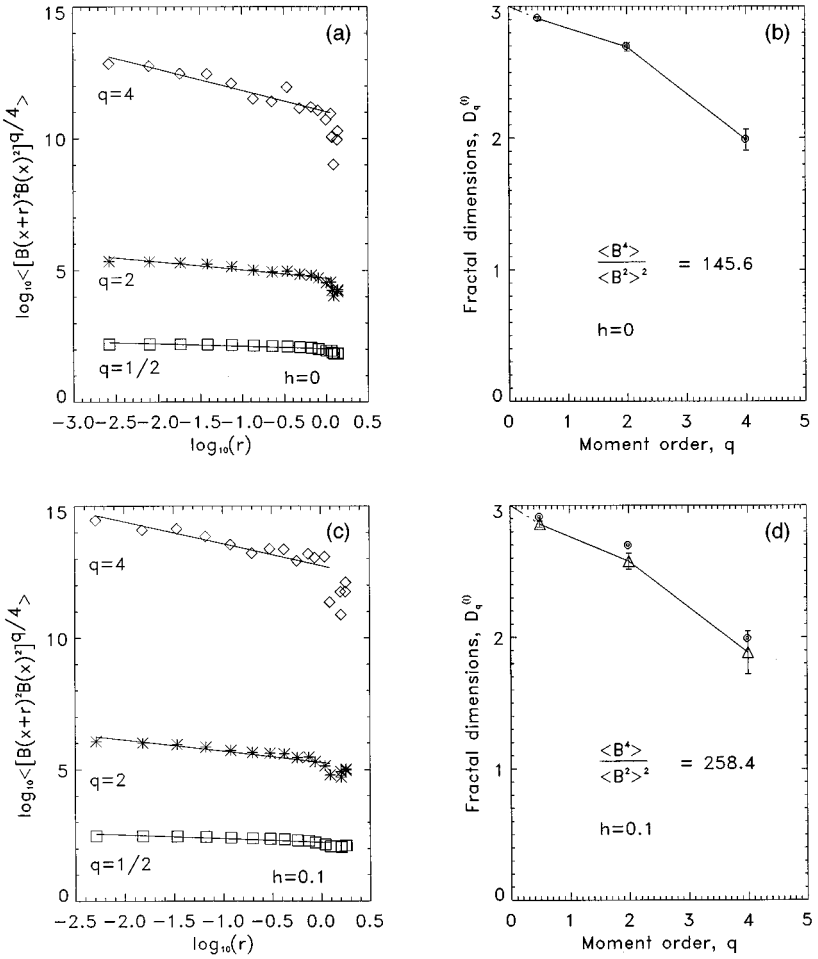

FIG. 8. Intermittency fractals, for two different initial locations of a field line. (a) Scaling after six STF cycles, for $h=0$. (b) Dimension spectrum, for $h=0$. Panels (c) and (d) repeat (a) and (b), for the case $h=0.1$. The dimension spectra for the two cases are rather similar [which can be seen directly in (d), in which the dimension spectrum from (b) is superimposed on the $h=0.1$ spectrum]; there is some slight evidence that the generalized dimensions for the $h=0.1$ case are smaller, implying that this case is somewhat more singular.

In Fig. 9(c), we display the evolution of $(l/\delta)^2$ with time; as we will discuss below, this quantity is closely related to the effective magnetic Reynolds number R_m. We see that the characteristic spatial scale decreases exponentially with time,

$$(l/\delta)^2 \sim e^{1.58t}.$$

Inspection of Fig. 9(c) also shows that this spatial scale reduction is less rapid than the magnetic field growth (which is also exponential in time, but with a larger growth rate). This situation is typical for dynamos [1].

Formally, we know that the magnetic Reynolds number for our problem is infinite (because the nature of the Lundquist solution presumes zero diffusivity); and we further know that for the STF problem, one ''classically'' would not expect to see spatial scale reduction [i.e., one would classically expect that $n=0$ in Eq. (1)]. However, as we have just seen, spatial scale reduction does occur in our calculations, and it is therefore appropriate to consider an effective Reynolds number R_m, and to determine its value. In order to define this quantity, we go back to our earlier discussion of small-scale dynamos (Secs. I and II), where we noted that the magnetic field scale is reduced until it reaches the scale of the exponentially fastest-growing eigenfunction of the kinematic problem, i.e., the diffusive scale δ [11]. Once the magnetic field scale has reached this value, this growing solution takes over, so that δ is the final characteristic scale of the magnetic field, i.e., the correlation scale is then of order δ. Now, since one would expect (for a finite Reynolds number) that $\delta=l/R_m^{1/2}$, one can define the effective magnetic Reynolds number as

$$R_m \equiv \left(\frac{l}{\delta}\right)^2. \tag{14}$$

This formula is *not* valid at the initial stage, when $\delta=l$, i.e., no scale reduction can occur at the initial stage by definition. What is more, if there were no scale reduction during successive STF cycles, Eq. (14) would be inappropriate because, again, $\delta=l$—leading to the result that the effective Reynolds number is $R_m=1$, while in contrast $R_m\to\infty$ as long as no scale reduction takes place. We can therefore apply formula (14) only because we do observe scale reduction, i.e., we observe that δ decreases exponentially as successive STF transformations are applied. [It is for this reason that we have denoted $(l/\delta)^2$ by R_m in Figure 9(c).]

The large-scale magnetic field component can be measured by averaging the long-range correlation function, thus defining $\langle B_0^2\rangle$; the result is also depicted in Fig. 9(c). We can see that the large-scale magnetic field energy by and large does grow with time, though not monotonically: roughly speaking, the large-scale component grows only on average, and at a rate distinctly slower than both the rate at which the magnetic field spatial scale is reduced, and the rate at which the small-scale component of the magnetic field increases:

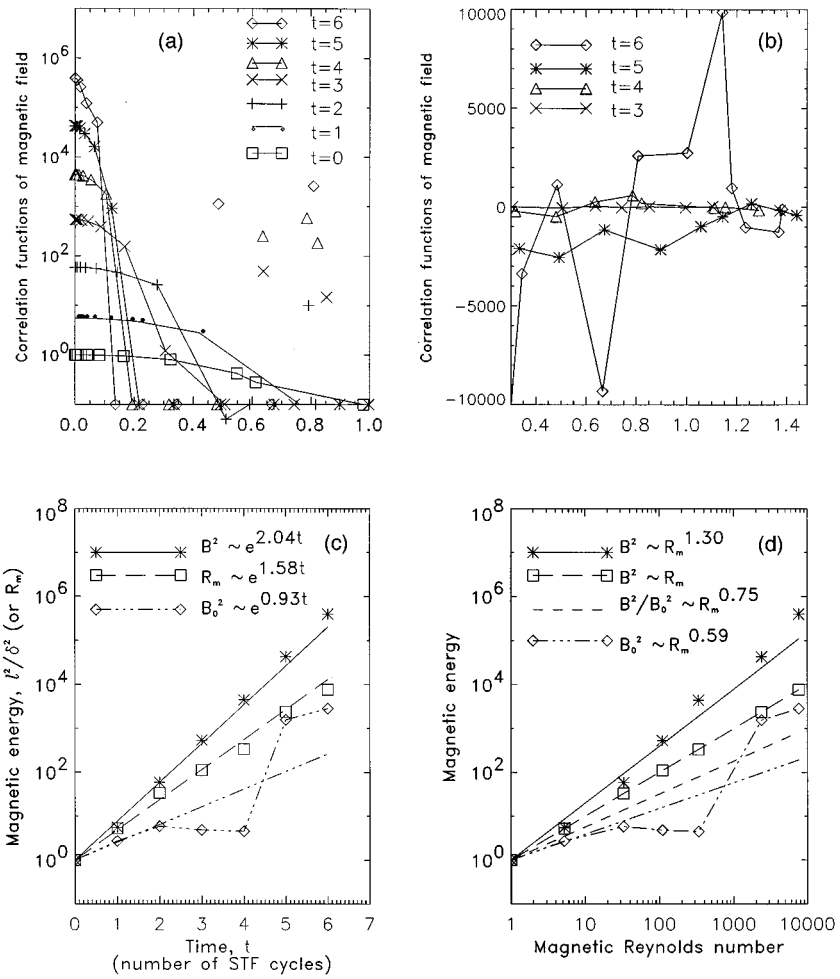

FIG. 9. Correlation properties of the magnetic field; in all cases, the initial line lies in the $z=0$ plane ($h=0$). (a) Correlation functions at different time steps. Because of exponential field growth, the ordinate is in logarithmic units, and therefore only positive portions of the correlation functions can be depicted. (b) Fluctuations of the ''tails'' of the correlation function, for different time steps, shown on a linear ordinate scale. (c) Magnetic energy amplification at small (asterisk) and large (diamond) scales, and growth of scale reduction, i.e., decrease of the correlation length δ (square). The latter quantity is computed by plotting $1/\delta^2$; as discussed in the text, this is equivalent to plotting the evolution of the effective Reynolds number R_m ($\sim 1/\delta^2$). (d) As (c), but all quantities are plotted vs the effective magnetic Reynolds number.

One can similarly consider the dependence of the small- and large-scale magnetic field components, and of the magnetic field spatial scale, on the effective Reynolds number R_m; these are shown in Fig. 9(d). From this analysis, we can determine n [in Eq. (1)], we find that $n=0.75$.

An obvious question is to what extent the results just discussed depend upon initial conditions. In order to answer this question, we have repeated the calculations leading to Fig. 9, but assuming that the initial magnetic field line is now at $z=h=0.1$; the results are shown in Fig. 10. We see once again exponential spatial scale reduction, and exponential growth of fluctuations. However, we do see one possibly significant difference from the earlier calculations: there is substantial decrease of the large-scale component at the very beginning i.e., after the first STF cycle. In order to understand this unexpected result, we have repeated this calculation for the first STF step only, but for an ensemble of 64^2 initial field lines, and have then computed the correlation functions for the resulting magnetic field at $t=0$ and at the $t=1$ step (i.e., after one STF transformation); the results are shown in Fig. 11. The result for $t=0$ is as expected, since we know that the total magnetic flux through (say) the $x=0$ plane must be zero initially (so that the magnetic field has to change sign). A rough measure of the large-scale magnetic field can be obtained by considering the following average of the correlation function:

$$\overline{C} \equiv \frac{1}{R_2 - R_1} \int_{R_1}^{R_2} C(r)\,dr,$$

where $C(r)$ is the correlation function, and the interval $R_2 - R_1$ is taken to be as large as possible; we take R_1 to be roughly equal to the value of the lag at which the initial correlation function has its first zero, and take R_2 to be the largest lag possible in our calculations. (Note that while the definition of R_2 is unambiguous, the definition of R_1 is somewhat arbitrary; in our experience, the precise value of R_1 is however not critical to the following discussion.) We then define

$$\langle B_0^2 \rangle \equiv |\overline{C}|.$$

It is clear from Fig. 11 that the negative portion of the correlation function at $t=1$, i.e., after the first STF stage, is certainly less than that of initial stage. In other words, the large-scale component definitely decreases after the first STF stage, confirming our earlier result for the single field line lying initially at $h=0.1$ [i.e., Fig. 10(c)]. Thus we can conclude that the behavior seen in Fig. 9(c) is actually anomalous (despite the fact that an increase in the large-scale field even after a single STF transformation is ''expected'' under the naive interpretation of the STF process): it is only a very special, ''favorite,'' field line that behaves as one classically expects.

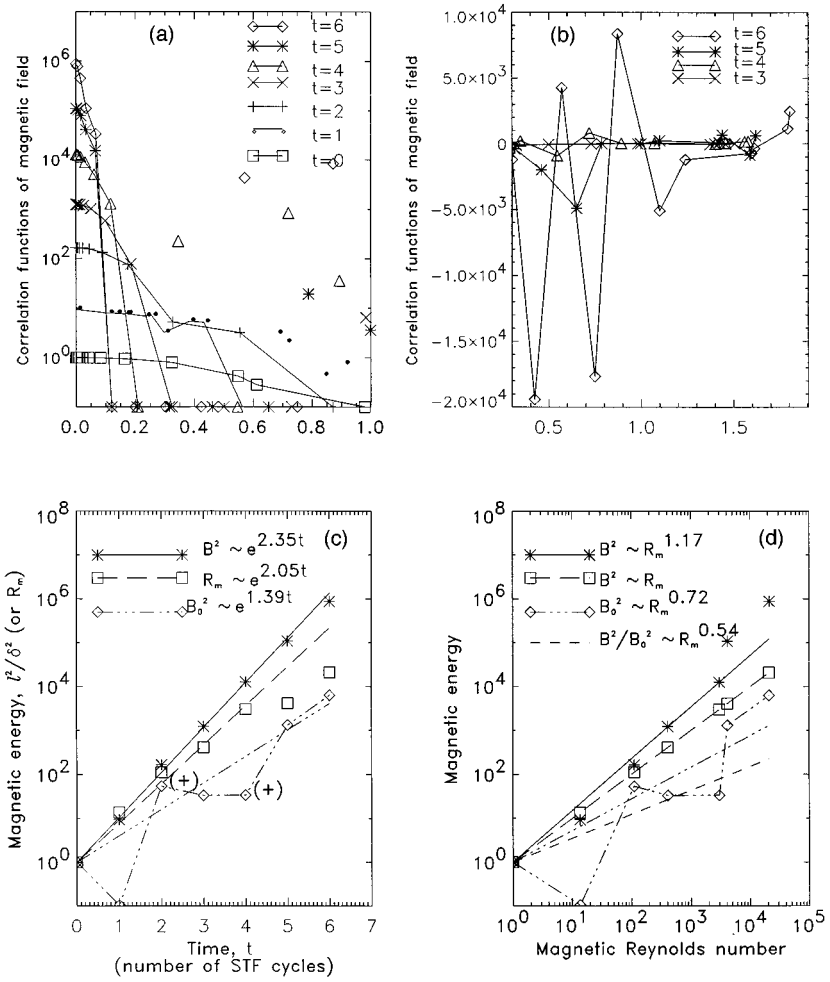

FIG. 10. Same as Fig. 9, except the initial line lies in the $z=0.1$ plane ($h=0.1$).

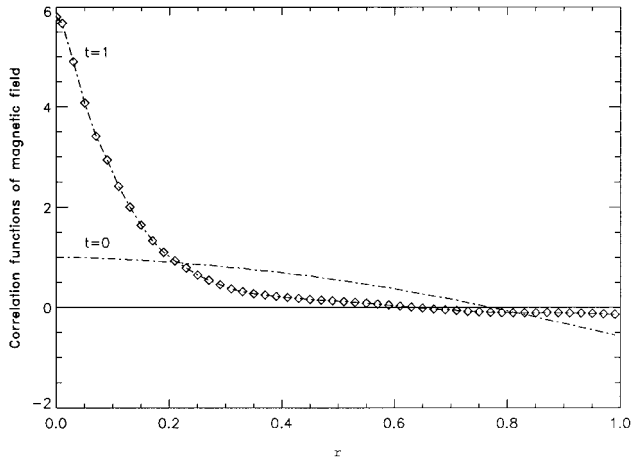

FIG. 11. Correlation functions for the initial state at $t=0$ (dot-dashed curve) and after one STF cycle (diamonds), computed for an ensemble of 64^2 magnetic lines. Note that the negative portion of the $t=1$ correlation function is smaller (in absolute magnitude) than the initial correlation function, implying that the large-scale magnetic field has actually decreased after this first step.

Another way to observe the variations of the large-scale magnetic field components is to construct a Poincaré section of the magnetic field corresponding to, for example, the $x=0$ plane. Figure 12 depicts two such sections after six STF cycles, for magnetic field lines lying initially in the $z=0$ and $z=0.1$ planes. We note first that there are no regions of continuous intersection, that is, there are no chaotic regions in the Poincaré sense; this is probably because we have constructed these sections after only six cycles. (We recall that, typically, continuous regions appear only for trajectories that pass the periodic cell a large number of times, which would be equivalent to many STF cycles in our case.) However, the Poincaré sections shown in Fig. 12 depict the sign of the field (and therefore may be referred to as ''polarized'' maps); that is, we distinguished the intersections of the plane with a magnetic field line by different symbols, depending on the direction of the field at the intersection point. Now, under the naive picture of the STF process, one would expect that most field lines would pierce the $x=0$ plane one way on the right-hand side of this plane, and the other way on the left-hand side; however, this is not observed. Instead, what we observe is fairly good mixing of the two field polarities; thus these polarized Poincaré maps imply that the large-scale magnetic field does not look like what was expected, confirming in a qualitative fashion the above quantitative conclusions drawn from an examination of the long-range behavior of the correlation functions.

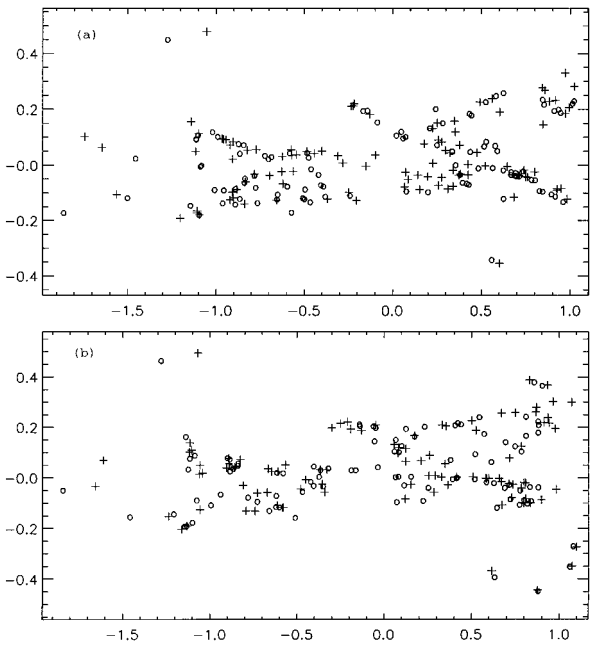

FIG. 12. Polarized Poincaré maps, or sections, for a single magnetic field line, after six STF cycles. (a) Initial line lies in the $z=h=0$ plane. (b) Initial line lies in the $z=h=0.1$ plane. Both plots correspond to intersection of the magnetic field line with the $x=0$ plane. Circles correspond to $B_x>0$, and plus signs to $B_x<0$. For an ''ideal'' STF cycle, all the circles would be on the right-hand side of the section plots, and plus signs on the left-hand side; clearly, the STF process studied here does not yield this expected result.

Returning to Fig. 10, we observe that [in panel (c)] the large-scale field component does eventually grow [as was seen in Fig. 9(c)]; and, similarly, the large-scale portion of the correlation function is *not* negative at the second and fourth stages [marked by (+) in panel (c)]. We conclude that the large-scale component does in fact grow on average; from the results shown in Fig. 10, we find that the average exponent is $2\gamma\sim1.387$, while the expected exponent due to doubling of the field is $2\ln2=1.386$. (The remarkable correspondence of these two numbers is most likely a coincidence, given the likely numerical errors.) Finally, from Fig. 10(d), we obtain $n=0.54$.

VI. CONCLUSIONS AND DISCUSSION

We have addressed the question of whether the stretch-twist-fold dynamo process should be considered as a prototype for the magnetic dynamo processes and, in particular, for ''large-scale'' dynamos. The first point is that because of the amplification of fluctuations, we find that the exponent n [from Eq. (1)] is not small; in fact $n>0.5$, as would be expected from simple geometrical considerations [25]. While numerical simulations cannot be considered as a proof of the existence of fluctuations, it is nevertheless clear that it is very difficult to ''tune'' the simple STF motion suggested by Moffatt and Proctor [11] in such a way that fluctuations do not appear. Indeed, fluctuations seem to be an inevitable by-product of the STF. Furthermore, as we saw in Secs. IV A and IV B, there are two unwanted effects accompanying the STF. First, only the ''favorite'' field line behaves as expected; the unwanted distortion of the other lines is probably inevitable. Second, there are side effects even for this ''good'' field line, as even this field line cannot be stretched-twisted-folded ''ideally.'' As a result, the field line becomes totally distorted after only a few cycles.

It is not known if there exists more complicated STF motions than suggested in [11] that would give no fluctuations. Our impression, derived from the study presented here, is that the geometric distortions (leading to rapid growth of fluctuations) are inevitable for any version of the STF motion. (We would therefore expect that any STF motion that does lead to ''ideal'' behavior is most likely structurally unstable; that is, only slight variations of the STF parameters would result in dramatic changes in the field line geometry.) As a result, we suggest that the previously held belief that the STF process is a prototype for a fast dynamo process, with the property that $n=0$ in Eq. (1), is most likely incorrect. That is, while our numerical study does not prove that $n\neq0$, we can assert that claims that $n=0$ cannot be taken at face value, but rather must be demonstrated.

Is the STF process a model for a large-scale dynamo? From Figs. 9 and 10, we would conclude that the answer is ''yes;'' however, these numerical results do not prove the possibility of such a dynamo. As for the small-scale dynamo process, we recall from Sec. V that the magnetic field on small scales grows faster than the rate at which the magnetic spatial scale is reduced; that is, field amplification is more effective than scale reduction. As the later process eventually leads to field dissipation, we may expect that, for the STF motion, dynamo action wins the battle against diffusion; that is, we expect that dynamo action will not saturate via diffusive processes, but more likely will saturate because of nonlinear processes which become important as the small-scale field grows, and the Lorentz back reaction takes effect. In any case, it would seem that the STF process does indeed lead to a magnetic dynamo.

Finally, an important issue for studies of the sort reported in this paper, namely those based on numerical simulations, is the effects of discretization and limited resolution; this issue has already emerged in our previous discussions when faced with the question of how long the Lundquist solutions may be followed in order to compute the STF line stretching. In particular, one may ask whether we could be making a mistake regarding the importance of the growth of small-scale fluctuations. Here we only wish to point out that our procedures insure that our estimates for this growth is conservative, i.e., our results *underestimate* the fluctuation growth rate. We have in fact compared results for line stretching for varying resolutions, and find that the fluctuations increase with increasing resolution. This is in fact to be expected: The accuracy with which the Lundquist solution provides the evolution of a given point on a given field line is independent of the resolution (but just depends upon the accuracy of the integration). In contrast, the rate of line stretching does depend upon resolution because our computation of the line length is based on approximating a line by a sequence of joined chords connecting sequential points on a field line; we obtain an underestimate of the line length because the chord joining sequential points is the shortest possible distance between these points.

Note added in proof. The evolution of the field line (Sec. IV) has been made in the first-order approximation. As we previously noted [18], the line was assumed to be well resolved if, at the last step, the distance between the neighbor points remains ''infinitesimal small,'' i.e., much less than the characteristic scale. S. Lantz (Cornell University) has suggested a scheme for calculating the field line correct to second order. Preliminary simulations confirm our expectation that the second-order corrections do not change our main results. First, they still show that only a few ''favorite'' field lines perform the STF, as expected, and most of them behave differently. Second, after a few (in fact, four) STF cycles, the line becomes chaotic.

Convergence was tested with assistance from Lantz. Comparing the two approximations, one finds a slight systematic deviation for these two cases; that is, there are small ($\sim$1% in average) large-scale geometric distortions, but no further small-scale structure is introduced. Such distortions are similar to those resulting from small changing in the parameters (given in Sec. III, and specified in the caption of Fig. 1). It appears interesting to study the effect of changing parameters (provided, of course, the motion still remains of STF type) on magnetic field statistics. We would not expect, however, a strong dependence on parameters because the statistical properties are robust, by definition.

ACKNOWLEDGMENTS

We thank A. Malagoli, who suggested programs to calculate the correlation functions, and assisted us with magnetic field line visualization. We also are grateful to N. Lebovitz, K. R. Sreenivasan, S. Childress, K. H. Moffatt, and E. N. Parker for their interest in this work and for discussions.

[1] S. I. Vainshtein and Ya. B. Zel'dovich, Usp. Fiz. Nauk **106**, 431 (1972) [Sov. Phys. Usp. **15**, 159 (1972)]; L. D. Landau and E. M. Lifshitz, *Electrodynamics of Continuous Media*, (Pergamon, New York, 1984), Sec. 74.

[2] S. Childress and A. D. Gilbert, *Stretch, Twist and Fold: Fast Dynamo* (Springer-Verlag, Berlin, 1995).

[3] See, e.g., B. J. Bayly, Phys. Rev. Lett. **57**, 2800 (1986); A. D. Gilbert and S. Childress, *ibid*. **65**, 2133 (1990).

[4] E. N. Parker, Astrophys. J. **122**, 293 (1955).

[5] Ya. B. Zel'dovich, Zh. Eksp. Teor. Fiz. **31**, 154 (1956) [Sov. Phys. JETP **4**, 460 (1957)].

[6] H. K. Moffatt, J. Fluid Mech. **11**, 625 (1961).

[7] R. H. Kraichnan and S. Nagarajan, Phys. Fluids **10**, 859 (1967).

[8] S. I. Vainshtein and R. Rosner, Astrophys. J. **376**, 199 (1991).

[9] The effective Reynolds number $\mathrm{Re}=ul/\nu$ and effective magnetic Reynolds number $R_m=ul/\eta$ are crucial control parameters in this problem, and are defined by the rms flow velocity u, the typical velocity scale length l, viscosity ν, and the magnetic diffusivity η.

[10] F. Cattaneo and S. I. Vainshtein, Astrophys. J. **376**, L21 (1991); R. M. Kulsrud and S. W. Anderson, *ibid*. **396**, 606 (1992); L. Tao, F. Cattaneo, and S. I. Vainshtein, in *Solar and Planetary Dynamos*, edited by M. R. E. Proctor, P. C. Matthews, and A. M. Rucklidge (Cambridge University Press, Cambridge, 1993); S. I. Vainshtein, L. Tao, F. Cattaneo, and R. Rosner, *ibid*; C. A. Jones and D. J. Galloway, *ibid*; A. V. Gruzinov and P. H. Diamond, Phys. Rev. Lett. **72**, 1651 (1994).

[11] H. K. Moffatt and M. R. E. Proctor, J. Fluid Mech. **154**, 493 (1985).

[12] S. I. Vainshtein, A. M. Bykov, and I. N. Toptygin, *Turbulence, Current Sheets and Shocks and Cosmic Plasma* (Gordon and Breach, New York, 1993).

[13] S. I. Vainshtein and F. Cattaneo, Astrophys. J. **393**, 165 (1992).

[14] A. D. Gilbert, N. F. Otani, and S. Childress, in *Solar and Planetary Dynamos* (Ref. [10]).

[15] H. K. Moffatt, *Magnetic Field Generation in Electrically Conducting Fluids* (Cambridge University Press, Cambridge, 1978).

[16] We change the order suggested in [11], making an ''eight'' *before* twisting the field, because otherwise this compression, being in the same plane as the loop, results in unexpected (and unwanted) strong distortion of the loop shape. Compression (7) proceeds in a different plane. Another feature is that the compression should act only at relative small values of x, and therefore (in order to avoid distortion of the shape) we introduced another parameter in the exponent so that the damping is anisotropic.

[17] The cx^2 ''ingredient'' pulls the loop out of the $y=0$ plane. However, there are unwanted side effects, discussed in more detail in Sec. IV B. The entire cycle works more effectively if the coefficient c is small, and if, *before* this fold stage, the loop is slightly shifted as a whole along the y axis; this preliminary motion accomplishes the job. We do not follow the next step suggested in [11], that is, to sum all the velocities into one velocity field (so that all the steps are carried out simultaneously). There are two reasons for this. First, the operators $\hat{S}$, $\hat{T}$, and $\hat{F}$ do not commute, and therefore changing the order, or applying them simultaneously, would not result in the STF transformation. Second, the velocity field which then results is steady, and, according to [11], the eigenfunctions should then be characterized by the diffusive scale δ; that is, the fluctuations would appear *a priori*. Indeed, preliminary simulations with this steady motion show that strong fluctuations do appear.

[18] We note here that in either set of calculations, our resolution criterion is that the distance between two neighboring points on a given field line must remain much smaller than the characteristic scale of the curve or, equivalently, much smaller than the characteristic scale of the imposed STF motion, which is taken to be unity.

[19] S. I. Vainshtein, R. T. Pierrehumbert, K. R. Sreenivasan, and Y. Du (unpublished).

[20] S. I. Vainshtein, K. R. Sreenivasan, R. T. Pierrehumbert, V. Kashyap, and A. Juneja, Phys. Rev. E **50**, 1823 (1994).

[21] H. G. E. Hentschel and I. Procaccia, Physica D **8**, 435 (1983).
[22] K. Bajer and H. K. Moffatt, J. Fluid Mech. **212**, 337 (1990).
[23] K. Bajer, H. K. Moffatt, and F. H. Nex, in *Topological Fluid Dynamics, Proceedings of the IUTAM Symposium*, edited by H. K. Moffatt and A. Tsinober (Cambridge University Press, Cambridge, 1990).
[24] M. N. Rosenbluth, R. Z. Sagdeev, J. B. Taylor, and G. M. Zaslavski, Nucl. Fusion **6**, 297 (1966).
[25] E. Ott and S. I. Vainshtein, in *Research Trends in Physics: Plasma Astrophysics, La Jolla International School for Physics Studies*, edited by R. Kulsrud, G. Burbidge, and V. Stefan (AIP, New York, 1996).